ACS Macro Letters

Letter

pubs.acs.org/macroletters

Precise Compositional Control and Systematic Preparation of Multimonomeric Statistical Copolymers

Jeffrey M. Ting,[†,‡] Tushar S. Navale,[†,§] Frank S. Bates,*[,‡] and Theresa M. Reineke*[,§]

Departments of [§]Chemistry and [‡]Chemical Engineering and Materials Science, University of Minnesota, Minneapolis, Minnesota 55455-0431, United States

Supporting Information

ABSTRACT: A comprehensive approach to target exact molecular weights and chemical compositions for multimonomeric statistical copolymers using a new controlled statistics method with reversible addition−fragmentation chain transfer free-radical (RAFT) polymerization is presented. The system chosen to illustrate this procedure is an acrylic quarterpolymer consisting of methyl acrylate, 2-carboxyethyl acrylate, 2-hydroxypropyl acrylate, and 2-propylacetyl acrylate, modeling a well-known macromolecule utilized to deliver poorly water-soluble drugs (hydroxypropyl methylcellulose acetate succinate, HPMCAS). The relative reactivities at 70 °C between monomer pairs were measured and employed to predict the feed ratio necessary for synthesizing well-defined compositions based on the Walling-Briggs model. Application of Skeist's equations addressed compositional drift and anticipated the general monomer incorporation distribution as a function of conversion, which was verified experimentally. This new and simple paradigm combining both predictive models provides complementary synthetic and predictive tools for designing macromolecular chemical architectures with hierarchical control over spatially dependent structure−property relationships for complex applications such as oral drug delivery.

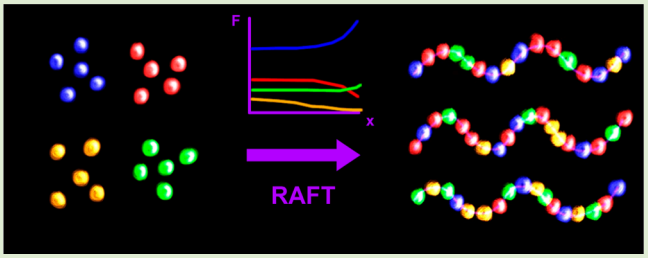

There is a growing interest in the polymer science landscape to access architecturally tailored[1] and sequence-specified[2] macromolecules to acquire enhanced properties. Structurally controlled polymers are of widespread importance across many diverse fields, from drug delivery[3] to photovoltaics[4] and microlithography.[5] In these and many other areas, statistical copolymers (SCPs) are often utilized. These compounds typically contain two or more monomers with desirable functionalities at specific composition, hinging on monomer concentration and reactivity that aids morphological control and imparts unique physical properties. For example, SCPs are playing an ever-increasing role in the storage, delivery, and approval process of poorly water-soluble active pharmaceutical agents, which encompass a significant portion of the current drug pipeline.[6] Interplay between the active molecule and the polymer matrix dictates drug solubility, controlled release, efficacy, and safety; this is particularly evident in an interesting cellulosic excipient platform referred to as hydroxypropyl methylcellulose acetate succinate (HPMCAS),[7] a randomly functionalized polymer that is chemically analogous to multimonomeric SCPs. While exceptionally effective compared to noncellulosic polymers in oral drug delivery,[8] the effects of its chemistry on promoting favorable drug interaction are poorly understood due to high material dispersity and difficulties in chemical characterization,[9] along with limited structure−function knowledge.[10] To this end, new synthetic methodologies to create multicomponent copolymers with tight control over variables such as molecular weight, chemical composition, etc. are needed to better understand the material function of HPMCAS and impart its properties toward the development of new polymeric excipients.

However, unlike many branches of chemistry[11] and biology[12] where architecture can be constructed judiciously on the molecular level, the stochastic nature of free-radical copolymerization results in a statistical distribution in length (molecular weight) and chemical composition, two crucial structural variables that govern overall functionality and performance. Methods to control SCP dispersities have been studied extensively for binary systems. "Living" (controlled) free-radical polymerization techniques, such as nitroxide-mediated polymerization (NMP),[13] atom transfer radical polymerization (ATRP),[14] and reversible addition−fragmentation chain transfer (RAFT),[15] offer direct routes to narrow molecular weight distributions. Chemical composition can be predicted with a terminal model, which assumes that the reactivity of a propagating chain is only contingent on the monomer at the growing end.[16] However, for controlled free-radical polymerizations, the cyclic activation/deactivation equilibria[17] can affect propagation kinetics, leading to differences in monomer consumption. Matyjaszewski has shown how the intermittent activation mechanism of ATRP introduces additional kinetic pathways that distort terminal model predictions.[18] For RAFT, this drawback is not as consequential.

Received: June 15, 2013
Accepted: August 1, 2013
Published: August 15, 2013

ACS Publications © 2013 American Chemical Society

Feldermann et al. have shown that once the main equilibrium predominates, the RAFT mechanism has minimal influence on copolymerization behavior.[19] Thus, RAFT appears ideal for reconciling control over both molecular weight and chemical composition for SCPs.

While synthesizing and understanding two-monomer systems have been a primary focus in the field, there is a growing need to expand beyond binary systems. Toward this prospect, we introduce the concept of "controlled statistics" for multicomponent systems, which we show to be instrumental in creating sophisticated SCPs with tunable properties and targetable length scales of intermolecular associations. To the extent of our knowledge, no comprehensive guidance on traversing the domain of multimonomeric copolymerization kinetics is available to date. Herein, we demonstrate a systematic approach for simultaneously controlling the molecular weight and chemical composition of multicomponent SCPs through a combinatorial use of relative reactivity measurements and chemical compositional modeling, combining both the Walling-Briggs and Skeist models to ultimately enable the rational design of unprecedented multicomponent systems.

A statistical quarterpolymer denoted P(MA-*stat*-CEA-*stat*-HPA-*stat*-PAA) was prepared (see Scheme 1) using the RAFT

Scheme 1. Synthesis of P(MA-*stat*-CEA-*stat*-HPA-*stat*-PAA) via RAFT Polymerization

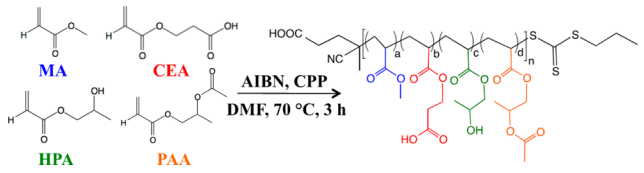

polymerization technique with four acrylic monomers: methyl acrylate (MA), 2-carboxyethyl acrylate (CEA), 2-hydroxypropyl acrylate (HPA, a mixture of isomers shown in the Supporting Information), and 2-propylacetyl acrylate (PAA). These monomers are amenable to RAFT chemistry and encompass chemical characteristics of HPMCAS that may yield interesting associative and mechanical properties for oral drug delivery arising from steric hindrance, hydrophilicity, ionizability, and hydrogen bonding.[20] RAFT polymerizations were conducted at 70 °C with the initiator 2,2′-azo-bisisobutyronitrile (AIBN) and chain transfer agent (CTA) 4-cyano-4-(propylsulfanylthiocarbonyl) sulfanylpentanoic acid (CPP) in dimethylformamide (DMF; see Supporting Information).

As with any free-radical polymerization process, it is important to first determine all of the monomer relative reactivities, or relative probabilities of monomer self-propagation over cross-propogation.[21] We investigated the conventional free-radical copolymerization of MA, CEA, HPA, and PAA in pairwise combinations to measure reactivity ratios at 70 °C. We conducted eight experimental runs for each pair, keeping the mole fraction of monomers in the feed (f_i) between 0.10 and 0.90 at a total monomer conversion below 15%. After calculating the total monomer conversion, the polymer composition (F_i) was determined using ^{1}H NMR (see Supporting Information). Figure 1 shows a plot based on the Mayo–Lewis relationship,[22] along with nonlinear fits to the experiments (eq 1), producing the reactivity ratios between MA with HPA and CEA with HPA at 70 °C. Table 1 contains the

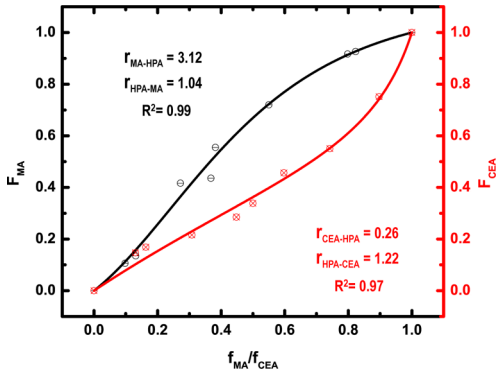

Figure 1. Reactivity ratio determination of MA with HPA (denoted in black) and CEA with HPA (denoted in red) with a nonlinear fit $F_1 = (r_{12}f_1^2 + f_1f_2)/(r_{12}f_1^2 + 2f_1f_2 + r_{21}f_2^2)$ in free-radical polymerization at 70 °C in DMF.

calculated reactivity ratios for all pairwise combinations between MA, CEA, HPA, and PAA.

$$F_1 = (r_{12}f_1^2 + f_1f_2)/(r_{12}f_1^2 + 2f_1f_2 + r_{21}f_2^2) \quad (1)$$

Table 1. Reactivity Ratios for Monomer Pairs[a] between MA, CEA, HPA, and PAA Polymerized at 70 °C

monomer	MA	CEA	HPA	PAA
MA		0.71	3.12	0.30
CEA	1.31		0.26	1.28
HPA	1.04	1.22		0.83
PAA	0.81	1.09	1.34	

[a]Reactivity ratio r_{ij} denoted by monomer i (row) to j (column).

We employed the four-component Walling-Briggs copolymerization model[23] to target specific polymer chemical compositions at low conversion, shown in Figure 2a. This model incorporates the monomer feed and reactivity ratios to predict the resultant polymer chemical composition. The system of equations for the Walling-Briggs model was solved numerically with Mathematica.[24] Two RAFT experiments with a degree of polymerization (DP = $[M]_0/[CTA]$) of 250 were

(a)

$$\left[\begin{array}{l} \dfrac{F_1}{F_2} = \dfrac{f_1D_1\left(f_1 + \dfrac{f_2}{r_{12}} + \dfrac{f_3}{r_{13}} + \dfrac{f_4}{r_{14}}\right)}{f_2D_2\left(\dfrac{f_1}{r_{21}} + f_2 + \dfrac{f_3}{r_{23}} + \dfrac{f_4}{r_{24}}\right)} \\ \dfrac{F_1}{F_3} = \dfrac{f_1D_1\left(f_1 + \dfrac{f_2}{r_{12}} + \dfrac{f_3}{r_{13}} + \dfrac{f_4}{r_{14}}\right)}{f_3D_3\left(\dfrac{f_1}{r_{31}} + \dfrac{f_2}{r_{32}} + f_3 + \dfrac{f_4}{r_{34}}\right)} \\ \dfrac{F_1}{F_4} = \dfrac{f_1D_1\left(f_1 + \dfrac{f_2}{r_{12}} + \dfrac{f_3}{r_{13}} + \dfrac{f_4}{r_{14}}\right)}{f_4D_4\left(\dfrac{f_1}{r_{41}} + \dfrac{f_2}{r_{42}} + \dfrac{f_3}{r_{43}} + f_4\right)} \\ F_1 + F_2 + F_3 + F_4 = 1 \end{array}\right]$$

(b)

$$\left[\begin{array}{l} \dfrac{\partial f_1}{\partial x} = \dfrac{F_1 - f_1}{x - 1} \\ \dfrac{\partial f_2}{\partial x} = \dfrac{F_2 - f_2}{x - 1} \\ \dfrac{\partial f_3}{\partial x} = \dfrac{F_3 - f_3}{x - 1} \\ \dfrac{\partial f_4}{\partial x} = \dfrac{F_4 - f_4}{x - 1} \end{array}\right]$$

Figure 2. Four-component system of equations for the (a) Walling-Briggs model with instantaneous polymer mole fraction F_i, monomer mole fraction f_i, reactivity ratio r_{ij}, and determinant D_i, as described in the original publication[23] (where $i, j = 1–4$), and the (b) Skeist model with the instantaneous change in f_i over the total monomer conversion x.

dx.doi.org/10.1021/mz4003112 | ACS Macro Lett. 2013, 2, 770–774

Table 2. Comparison of Theoretical Walling-Briggs and Experimental Polymer Compositions

run	conv.[a]	$M_{n,\,calc}$[b] (kg/mol)	$M_{n,\,exp}$[c] (kg/mol)	$Đ$[d]	%mol monomer feed (MA/CEA/HPA/PAA)	%mol polymer$_{theo}$ (MA/CEA/HPA/PAA)	%mol polymer$_{exp}$[f] (MA/CEA/HPA/PAA)
1	0.23	7.9	7.9	[e]	13/70/12/5[d]	10/60/25/5	10/67/16/7
2	0.44	11.0	11.7	1.09	67/22/8/3[d]	60/25/10/5	61/27/10/3

[a]Determined from ^{1}H NMR of the reaction mixture. [b]$M_{n,calc}$ = (sum of monomer molecular weight times measured experimental polymer composition) × (conversion) × (DP). [c]Calculated based on end-group analysis from ^{1}H NMR assuming one CTA end group per chain. [d]Determined by SEC light scattering using tetrahydrofuran (THF) as the eluent at 25 °C with a measured dn/dc of 0.0676 mL/g. [e]Unavailable due to insolubility in THF. [f]Calculated from ^{1}H NMR of the isolated polymer.

conducted to illustrate the use of this model, shown in Table 2. In both instances, the monomer feed ratio was predetermined based on the desired polymer composition at low conversion. For both runs, isolated polymer compositions measured with ^{1}H NMR corroborated predictions from the Walling-Briggs model. For example, to synthesize a polymer with M_n = 11.0 kg/mol (run 2), the polymerization was stopped at 44% total monomer conversion. ^{1}H NMR end group and size exclusion chromatography (SEC) analyses (M_n = 11.7 and 11.4 kg/mol, respectively) were found to be in agreement, and the actual composition (62/28/8/2 mol % of MA/CEA/HPA/PAA) was close to the Walling-Briggs prediction.

The practical utility of this procedure depends on addressing two fundamental issues: for a given system (1) over what "limited" conversion does the Walling-Briggs model remain predictive and (2) when does compositional drift become detrimental to chemical homogeneity or end-group fidelity? High monomer conversion reduces product purification costs and minimizes waste. Optimal production strategies must ultimately include these factors.

Free-radical polymerization inherently is an unsteady-state process, where monomer and initiator concentrations change as the polymerization proceeds. There is a trade-off between higher yields and maintaining compositional control, as first discussed by Skeist, who related compositional drift to the classic Rayleigh problem for a simple binary distillation.[25] Skeist's equations anticipate changes in the instantaneous polymer composition with total monomer conversion and tracks compositional drift, which can reveal subtle variations in the associated chemical microstructure. For binary systems, the polymer structure is directly tied to the monomer reactivity ratios. For instance, a MA-HPA (denoted 1−3, with r_{13} = 3.12, r_{31} = 1.04) copolymerization yields a gradient copolymer because polymer chains with terminal MA end groups undergo self-propagation approximately three times faster than cross-propagation toward HPA monomers, while chains with terminal HPA end groups have approximately equal preference for self- and cross-propagation. However, the reaction dynamics and resulting copolymer structure of systems with three or more monomers is less transparent due to potential complex couplings between the underlying binary reactivity ratios. For multicomponent systems, the Skeist approach provides a simple tool to account for the network of reactions that describes the instantaneous state of polymerization at any time during a batch polymerization. Alternatively, monomers can be added to the reactor continuously during a polymerization, which manages compositional drift directly,[26] but introduces additional control, modeling, and equipment complexity.

For our system, four coupled nonlinear ordinary differential equations describe the instantaneous polymer chemical composition versus the total monomer conversion (Figure 2b). We computed the results associated with runs 1 and 2 (Table 2) in Matlab[27] using ODE 45, a standard numerical solver employing a Runge−Kutta integration method with variable time steps. The results for run 2 are shown in Figure 3,

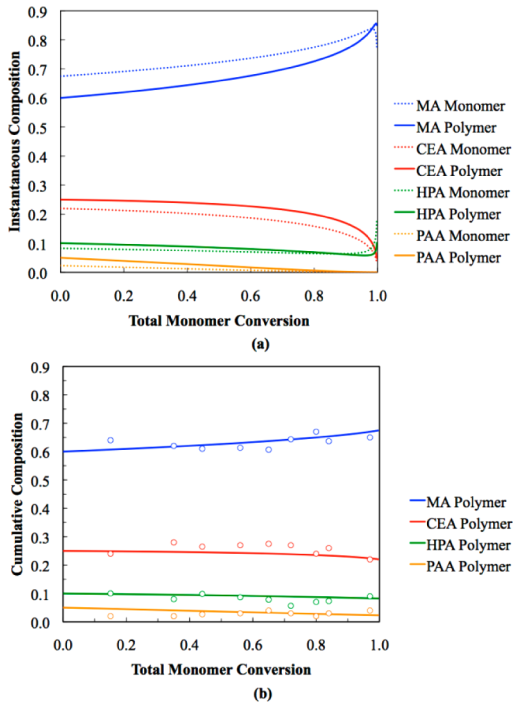

Figure 3. Comparison of (a) instantaneous and (b) cumulative chemical composition vs conversion for a targeted [MA/CEA/HPA/PAA] = [0.60/0.25/0.10/0.05] polymer composition (run 2). Dotted and solid lines represent the predicted monomer and polymer compositions, respectively. Open circles describe experimental data points of the average polymer composition, determined by ^{1}H NMR.

while run 1 is discussed in the Supporting Information. Figure 3a illustrates the predicted instantaneous polymer composition as a function of monomer conversion. As the polymerization proceeds, preferential addition of MA monomers and a bias against adding PAA monomers shifts the instantaneous composition away from the distribution at low conversion. To ensure reasonable chemical homogeneity this reaction should be quenched before 60% conversion to maintain statistical placement of PAA monomers throughout the polymer. These snapshots of the monomer and polymer compositions during a polymerization are essential in designing reactions that produce prescribed levels of randomness or blockiness in SCPs. Alternative methods to quantify the monomer sequence distribution, such as ^{13}C NMR spectroscopy, have been developed,[28] but such techniques are challenging to apply to multicomponent systems.

dx.doi.org/10.1021/mz4003112 | ACS Macro Lett. 2013, 2, 770−774

Integration of the instantaneous polymer and monomer compositions up to a specified total monomer conversion leads to the cumulative compositions as illustrated for the statistical quarterpolymer in Figure 3b. We conducted several reactions following the procedure described above, taking aliquots every 15 min that were subjected to quantitative ^{1}H NMR analysis (see Supporting Information). At low conversions (<35%) the predicted polymer compositions were in close agreement with the experimental results (deviations associated with the pre-equilibration time in the RAFT mechanism[29] do not appear to significantly confound the free-radical terminal model kinetics). At higher conversions monomer depletion and potential loss of end-group fidelity could limit the model's overall accuracy. Moreover, the integrated composition becomes relatively insensitive to variations in the instantaneous composition beyond 80% total monomer conversion. This makes characterization of the monomer sequence in a multimonomer SCP virtually impossible, reinforcing the importance of a predictive model. Nevertheless, the predictions by our model appear to be robust, reinforcing our conviction that well-defined multimonomeric SCPs can be generated using the RAFT technique and quantitatively modeled with the combined Walling-Briggs-Skeist approach.

In summary, we developed a generalized method for preparing multicomponent SCPs with uniform molecular weights and well-defined chemical compositions. The acrylic quarterpolymer served as a model system to demonstrate the process of determining the pairwise monomer reactivity ratios, targeting specific polymer compositions, and identifying compositional drift. This ensures that any multicomponent polymeric system can be constructed in a facile, systematic manner. Additionally, because the polymer chemical composition is contingent on the specificity of the RAFT CTA, further refinement of the modeling is underway. Homopolymerizations of each monomer reveal that the inhibition time for MA is nearly twice as long as the other acrylate monomers (see Supporting Information), which will affect polymers synthesized at low conversion. Study of this overall pre-equilibration time is currently being investigated to combine these initial kinetic reaction pathways into the Walling-Briggs-Skeist model. Furthermore, incorporating mixtures of monomer families (e.g., acrylates, methacrylates, styrenics) that have more vastly different reactivity ratios can allow us to better examine these small but important details for the universality of our model. This will provide new insight into the details of the RAFT polymerization mechanism such as intermediate fragmentation kinetics or retardation effects from cross-termination for a selected RAFT agent.[30] Altogether, this methodology of utilizing controlled statistics will be useful for many applications, including designing multicomponent SCP excipients that imitate HPMCAS for oral drug delivery. Precise control of these HPMCAS analogs will allow physiochemical properties to be tailored for the storage and delivery of various poorly water-soluble active pharmaceutical ingredients. Thus, developing strategic control over all aspects of multicomponent copolymers will permit the study of structure−property relationships that enhance drug bioavailability and safety.

■ ASSOCIATED CONTENT

Supporting Information

Experimental details, characterization data, and figures referred to in the text. This material is available free of charge via the Internet at http://pubs.acs.org.

■ AUTHOR INFORMATION

Corresponding Author

*E-mail: bates001@umn.edu; treineke@umn.edu.

Author Contributions

†These authors contributed equally to this work.

Notes

The authors declare no competing financial interest.

■ ACKNOWLEDGMENTS

This material is based upon work supported by the National Science Foundation Graduate Research Fellowship under Grant No. 00006595. We thank The Dow Chemical Company for funding of this project. We would also like to thank Prof. Marc A. Hillmyer and Prof. Timothy P. Lodge at the University of Minnesota, as well as Steve Guillaudeu and Bob Schmitt at The Dow Chemical Company, for helpful discussions.

■ REFERENCES

(1) Bates, F. S.; Hillmyer, M. A.; Lodge, T. P.; Bates, C. M.; Delaney, K. T.; Fredrickson, G. H. *Science* **2012**, *336*, 434−440.

(2) (a) Badi, N.; Lutz, J. *Chem. Soc. Rev.* **2009**, *38*, 3383−3390. (b) Lutz, J. *Polym. Chem.* **2010**, *1*, 55−62. (c) Ganesan, V.; Kumar, N. A.; Pryamitsyn, V. *Macromolecules* **2012**, *45*, 6281−6297. (d) Powers, W.; Ryu, C. Y.; Jhon, Y. K.; Strickland, L. A.; Hall, C. K. *ACS Macro Lett.* **2012**, *1*, 1128−1133.

(3) (a) Euliss, L. E.; DuPont, J. A.; Gratton, S.; DeSimone. *Chem. Soc. Rev.* **2006**, *35*, 1095. (b) Gillies, E. R.; Fréchet, J. M. J. *Pure Appl. Chem.* **2004**, *76*, 1295−1307.

(4) (a) Yang, X.; Loos, J. *Macromolecules* **2007**, *40*, 1353−1362. (b) Chen, C.; Chan, S.; Chao, T.; Ting, C.; Ko, B. *J. Am. Chem. Soc.* **2008**, *130*, 12828−12833.

(5) (a) Bates, C. M.; Strahan, J. R.; Santos, L. J.; Mueller, B. K.; Bamgbade, B. O.; Lee, J. A.; Katzenstein, J. M.; Ellison, C. J.; Willson, C. G. *Langmuir* **2011**, *27*, 2000−2006. (b) Chen, W. C.; Chuang, Y.; Chiu, W. Y. *J. Appl. Polym. Sci.* **2001**, *79*, 853−863.

(6) Mullard, A. *Nat. Rev.* **2012**, *11*, 91−94.

(7) (a) Friesen, D. T.; Shanker, R.; Crew, M.; Smithey, D. T.; Curatolo, W. J.; Nightingale, J. A. S. *Mol. Pharmaceutics* **2008**, *5*, 1003−1019. (b) Ilevbare, G. A.; Liu, H.; Edgar, K. J.; Taylor, L. S. *Cryst. Growth Des.* **2012**, *6*, 3133−3143.

(8) Curatolo, W.; Nightingale, J. A.; Herbig, S. M. *Pharm. Res.* **2009**, *26*, 1419−1431.

(9) Chen, R.; Ilasi, N.; Sekulic, S. S. *J. Pharm. Biomed. Anal.* **2011**, *56*, 743−748.

(10) Grasman, N.; Porter III, W.; Petermann, O.; Brackhagen, M.; Guillaudeu, S.; Murri, B.; Miller, W.; Morgan, R.; Morgen, M. Impact of Substitution Level on Spray Dried Dispersions of Hypromellose Acetate Succinate—A Quality by Design Approach. In AAPS National Meeting, Chicago, IL, Oct 14−18, 2012, AAPS: Arlington, VA, 2012.

(11) Yang, L.; Shan, S.; Loukrakpam, R.; Petkov, V.; Ren, Y.; Wanjala, B. N.; Engelhard, M. H.; Luo, J.; Yin, J.; Chen, Y.; Zhong, C. *J. Am. Chem. Soc.* **2012**, *134*, 15048−15060.

(12) Hackel, B. J.; Wittrup, K. D. *Protein Eng. Des. Sel.* **2010**, *23*, 211−219.

(13) Hawker, C. J.; Bosman, A. W.; Harth, E. *Chem. Rev.* **2001**, *101*, 3661−3688.

(14) Wang, J. S.; Matyjaszewski, K. *J. Am. Chem. Soc.* **1995**, *117*, 5614−5615.

(15) Moad, G.; Rizzardo, E.; Thang, S. H. *Aust. J. Chem.* **2009**, *62*, 1402−1472.

(16) Mayo, F. R.; Lewis, F. M. *J. Am. Chem. Soc.* **1944**, *66*, 1594−1601.

(17) Moad, G.; Rizzardo, E.; Thang, S. H. *Acc. Chem. Res.* **2008**, *41*, 1133−1142.

(18) Matyjaszewski, K. *Macromolecules* **2002**, *35*, 6773−6781.

(19) Feldermann, A.; Ah Toy, A.; Phan, H.; Stenzel, M. H.; Davis, T. P.; Barner-Kowollik, C. *Polymer* **2004**, *45*, 3997−4007.
(20) (a) Kim, B. K.; Shin, J. H. *Colloid Polym. Sci.* **2002**, *280*, 716−724. (b) Lu, D.; Xie, J.; Shen, L.; Zhao, Q.; Yuan, T.; Guan, R. *J. Appl. Polym. Sci.* **2012**, *125*, 2807−2813. (c) Hoogenboom, R.; Popescu, D.; Steinhauer, W.; Keul, H.; Möller. *Macromol. Rapid Commun.* **2009**, *30*, 2042−2048.
(21) Alfrey, T.; Goldfinger, G. *J. Chem. Phys.* **1944**, *12*, 322.
(22) Odian, G. *Principles of Polymerization*, 4th ed.; John Wiley & Sons, Inc.: Hoboken, NJ, 2004; p 481.
(23) Walling, C.; Briggs, E. R. *J. Am. Chem. Soc.* **1945**, *67*, 1774−1778.
(24) *Mathematica*, version 8.0.4.0; Wolfram Research, Inc.: Champaign, IL, 2011.
(25) Skeist, I. *J. Am. Chem. Soc.* **1946**, *68*, 1781−1784.
(26) Kreft, T.; Reed, W. F. *Macromolecules* **2009**, *42*, 5558−5565.
(27) *MATLAB*, version 7.13.0.564, The Mathworks, Inc.: Natick, MA, 2011.
(28) Hunley, M. T.; Sari, N.; Beers, K. L. *ACS Macro Lett.* **2013**, *2*, 375−379.
(29) Keddie, D. J.; Moad, G.; Rizzardo, E.; Thang, S. H. *Macromolecules* **2012**, *45*, 5321−5342.
(30) (a) Meiser, W.; Barth, J.; Buback, M.; Kattner, H.; Vana, P. *Macromolecules* **2011**, *44*, 2474−2480. (b) Ting, S. R. S.; Davis, T. P.; Zetterlund, P. B. *Macromolecules* **2011**, *44*, 4187−4193.